

Chiral Recognition with Room-Temperature Phosphorescence in Guest-Host Energy-Transfer Systems

Biao Chen,^{*,[a]} Wenhuan Huang,^[a] and Guoqing Zhang^{*,[a]}

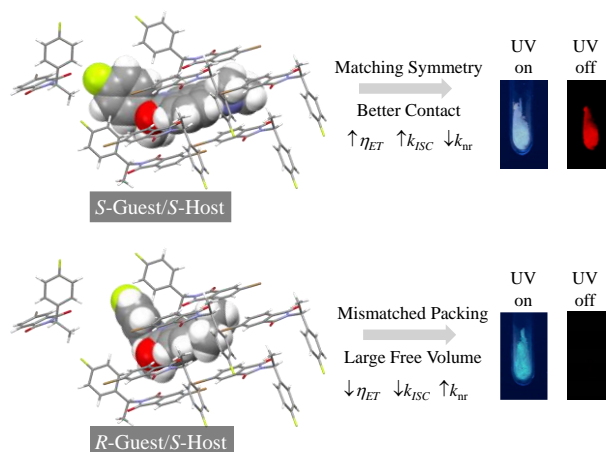
[a] Prof. B. Chen, Dr. W. Huang, Prof. G. Zhang
Hefei National Laboratory for Physical Science at the Microscale,
University of Science and Technology of China,
96 Jinzhai Rd, Hefei, Anhui 230026 (China)
E-mail: gzhang@ustc.edu.cn; biao chen@ustc.edu.cn.

Supporting information for this article is given via a link at the end of the document.

Abstract: Chiral recognition with molecular luminescence is a beneficial but challenging method due to an often lack of dramatic difference in intermolecular interactions between the chiral analyte/substrate pair versus their enantiomeric counterpart. Here we show that the difference in room-temperature phosphorescence (RTP) can be substantially augmented by employing guest-host energy-transfer systems. By covalent attachment of chiral amino compounds to a phthalimide host and a naphthalimide guest, respectively, RTP intensity difference of two orders of magnitude with a detection limit of >98% enantiomeric excess (ee) could be achieved. For example, S-enantiomeric guests in S-enantiomeric hosts produce strong red RTP afterglow while no appreciable RTP could be observed in an S/R guest-host combination. The huge spectroscopic difference in RTP results in conspicuous steady-state and delayed-emission variations, which could easily be discriminated by the naked eye. A generalized concept in solid-state RTP chiral recognition is proposed to expand the application scope of the reported method.

Chiral recognition^[1] is vital in pharmaceutical^[2] and life sciences, as is often the case where for a drug^[3] one enantiomer cures while the mirror-image other kills.^[4] Many techniques, including nuclear magnetic resonance (NMR), circular dichroism (CD), gas chromatography (GC), mass spectrometry (MS), and high-performance liquid chromatography (HPLC), have been developed to differentiate these isomers. Among these methods, photoluminescence-based enantiomeric discrimination^[5] is of interests in the past several decades as it is real-time, low-cost, and highly sensitive. Many luminescence chiral selectors based on 1,1'-bi-2-naphthol,^[6] tetraphenylethene,^[7] and polymers^[8] have been reported, with sensing modalities ranging from emission intensity to lifetime, and to color.^[9] Room-temperature phosphorescence (RTP), on the other hand, exhibits extra benefits, such as red-shifted wavelengths into the visible region and longer lifetimes^[10] for enantiomeric discrimination with higher sensitivity.^[11] RTP chiral selectors are usually rigid media such as inclusion complexes (e.g., cyclodextrin^[12]) or solid-state substrates^[13] (e.g., menthol) which are resistant to diffusing molecular oxygen and other quenchers, and the signal distinction, albeit scarce in examples, is subtle with only minor differences showing up in lifetimes between the two enantiomeric phosphors. The subtlety is not surprising since such a discrimination relies solely on the limited environmental disparity effects, which mainly dictate the difference in interactions between chemical groups of the analyte and substrate. Consequently, the key to success in RTP chiral recognition is to amplify such a disparity. Herein, we report a new RTP chiral recognition method by using an organic guest-host system consisting of a brominated phthalimide host and an

amino naphthalimide guest (Scheme 1), where the RTP intensity can be expressed by the following relationship: $I_{\text{RTP}} \propto \eta_{\text{ET}} \cdot k_{\text{ISC}} \cdot 1/k_{\text{nr}}$, where η_{ET} is the efficiency of excited-state energy transfer, k_{ISC} is the rate of intersystem crossing, and k_{nr} is the non-radiative decay rate. As Scheme 1 indicates, we expect that all three variables are related to chirality (e.g., spin polarization and orbital overlap during energy transfer) or chirality-related secondary effects (e.g., k_{nr} and k_{ISC} difference from presence or absence in close molecular contacts with external heavy-atom effects), so that amplification of the RTP intensity difference could be significant enough for the naked eye.



Scheme 1. Illustration of matching and mismatching molecular packing arrangements in guest-host systems of the same and different chirality, which potentially impact the RTP yield related to the efficiency of excited-state energy transfer η_{ET} , the rate of intersystem crossing k_{ISC} , and the non-radiative decay rate k_{nr} .

Two chiral amino compounds are chemically modified into naphthalimides **R-4FMNNI** and **S-4FMNNI** (Figure 1a), as guest molecules, and two host ones (**R-4FBrBI** and **S-4FBrBI**, Figure 1b), which are characterized by ¹H and ¹³C NMR spectra, high resolution mass spectrometry (HRMS, Figure S32-49), elemental analysis (EA) and chiral high-performance liquid chromatography (CHPLC). The CHPLC traces (Figure S1-S2, Table S1-S2) demonstrate that the model compounds are chiral molecules with high purity > 99.5% with ee values > 99.9%. Crystal parameters (Figure 1c) obtained from single-crystal X-ray diffraction (SC-XRD) reveal that these molecules exhibit the same monoclinic system, space group (*P*2₁), and similar dihedral angles between the phenyl and imide planes (109.28°–113.32°), suggesting high structural similarity in the solid state. The CD spectra (Figure S6) are used to determine their chirality

with absolute CD signal of 10-20 mdeg (0.1 mM). The absorption (Figure S5) and emission spectra (Figure S7) in dilute dichloromethane (CH_2Cl_2) show that **4FMNNI** set exhibit intense (Figure S7, Table S5) fluorescence while **4FBrBI** have no discernible emission, likely due to the heavy-atom effect.^[14] At 77 K, **4FBrBI** displays phosphorescence with a lifetime of several milliseconds, while **4FMNNI** exhibits no appreciable delayed emission (Figure S9), suggesting its low intrinsic phosphorescence yield.^[15]

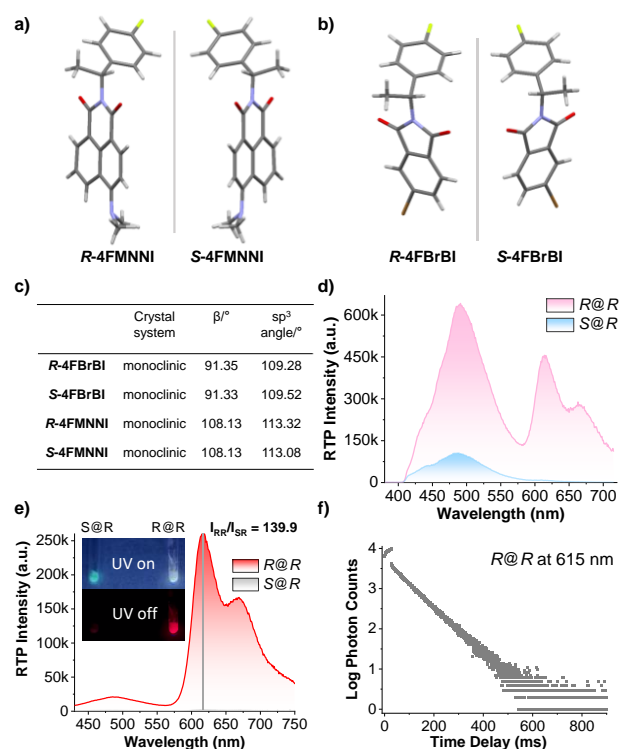


Figure 1. RTP Chiral recognition with $ef > 10^2$: a) Molecular configurations obtained from single-crystal X-ray diffraction (SC-XRD) for analyte guests **R-4FMNNI** and **S-4FMNNI**. b) SC-XRD structures for chiral selector hosts **R-4FBrBI** and **S-4FBrBI**. c) Crystal lattice parameters with α (90°) and γ (90°) omitted. d) Steady-state photoluminescence (PL) spectra of two chiral guests (w/w 10 ppm, pink for **R-4FMNNI** and light blue for **S-4FMNNI**) in the **R-4FBrBI** chiral selector host solid at 298 K ($\lambda_{\text{ex}} = 365$ nm). e) Delayed emission (DE, $\Delta t = 0.1$ ms) spectra of two chiral guests (w/w 10 ppm) in the **R-4FBrBI** solid at 298 K ($\lambda_{\text{ex}} = 424$ nm). Inset: photographs of combinations of two guests in **R-4FBrBI** during and immediately after 365-nm light irradiation. f) Time-resolved RTP emission at 615 nm for **R-4FMNNI** in solid **R-4FBrBI** at a concentration of 10 ppm.

The chiral selector **R-4FBrBI** was first examined as a solid-state host: cyan fluorescence (circa 491 nm, $\tau = 3.62$ ns) and red RTP (circa 615 nm) arise simultaneously constituting a visibly white emission color when **R-4FMNNI** (10 ppm, w/w, see SI for detailed protocols) is mixed with the selector medium (R@R, Figure 1d). Surprisingly, when its enantiomer (**S-4FMNNI**) is applied to the **R-4FBrBI** selector, only fluorescence occurs with no distinguishable RTP. Delayed emissions (DE) show that the enantiomeric RTP enhancement ratio ($ef = I_{\text{RR}}/I_{\text{SR}}$) is 139.9 (Figure 1e), with an R@R RTP lifetime of 73.31 ms (Figure 1d, Table 1). Subtraction of the background host signal from the total RTP gives an ef_{Δ} ($\Delta I_{\text{RR}}/\Delta I_{\text{SR}} = [I_{\text{RR}} - I_{\text{R}}]/[I_{\text{SR}} - I_{\text{R}}]$) of 196.6 (Figure S10). The achieved RTP chiral recognition via organic chiral solids (OSC), which is essentially an “on-off” mode.

DE spectra excited with 365-nm light display lower ef values due to host RTP interference (Figure S10 and S12-14). The selector host **S-4FBrBI**, the enantiomer of **R-4FBrBI**, can also achieve enantioselectivity as shown in Figure S11, where a “mirror-image relation” of RTP responses is observed toward the enantiomers of the **4FMNNI**, i.e., $ef(I_{\text{SS}}/I_{\text{RS}}) = 155.3$ with an RTP lifetime of 70.55 ms for S@S confirms the consistency of the chiral recognition method using the guest-host system.

Table 1. Photoluminescence properties of dopant samples (w/w 10 ppm) and pure host solids at room temperature.

Samples ^[a]	F max (nm) ^[b]	Lifetime (ns) ^[c]	P max (nm) ^[d]	Lifetime (ms) ^[e]	ef ^[f]
R@R	491	3.62	615	73.31	139.9
S@R	489	6.22	618	44.79	
S@S	481	5.41	617	70.55	155.3
R@S	483	5.50	618	41.94	
R-4FBrBI	/[g]	/	482	0.62	/
S-4FBrBI	/	/	482	0.85	/

[a] Guest-host molecular solids (w/w 10 ppm). [b] Fluorescence emission maxima of steady-state photoluminescence spectra excited at 365 nm. [c] Apparent fluorescence lifetime (Weighted average sum, naanoLED-370). [d] RTP maxima of delayed emission spectra excited at 424 nm. [e] Apparent RTP lifetime (spectraLED-370). [f] enantiomeric RTP enhancement ratios (ef_{RTP} , $I_{\text{SS}}/I_{\text{RS}}$ or $I_{\text{RR}}/I_{\text{SR}}$). [g] Not exist.

The guest/host ratio and its influences on enantioselectivity were then investigated. The PL spectra were presented in Figure 2a and Figure S17: when the host and the guest possess the same chirality (i.e., R@R or S@S), dramatically stronger RTP in the wavelength range of 600-720 nm emerges compared to samples of different chiralities (S@R or R@S), resulting in ef typically > 10 . The ef value of a guest-host doping of 0.1% is found to be < 3 because of intense guest fluorescence extending to the red region and elevating the baseline. On the other hand, S@R (or R@S) also exhibits appreciable RTP intensity when doped at high concentrations (> 100 ppm), possibly from guest aggregates formation^[16] or contribution from the enantiomeric impurity limited by current instrument detections. The highest ef is obtained in a doping ratio range of 1 to 100 ppm (e.g., $ef > 55$ for the 10-ppm sample), which is consistent with the DE spectra (Figure 2b-2d). Furthermore, the DE spectra present higher ef values (from 24.5 to 155.3 when guest/host ratio 1 ppm-100 ppm) than steady-state PL via eliminating short-lived luminescence interference (e.g., guest fluorescence and host phosphorescence), showcasing the prominent advantage from RTP chiral recognition. We found that the guest doping concentration of 1 ppm is sufficient for an highly enantioselective RTP enhancement of 24.5-32.0 folds, while many chiral recognition methods such as enantioselective fluorescence enhancement^[17] demands that the enantiomer analyte be at least in equal proportion or dozens of times in excess to the chiral selector^[18] With its high sensitivity, the guest-host RTP recognition method could be applied to ultratrace chiral analysis. Notably, samples with an identical chirality (S@S or R@R) present excitation-dependent PL emission (Figure S18-21): the fluorescence intensity increases while the RTP intensity barely changes with different excitation wavelengths (from 320 nm to

424 nm), leading to a divergent P/F ratio (Figure S18-20 d). Specially, in the 350-380 nm range, the P/F ratio decreases as the guest absorbance increases (Figure S5).

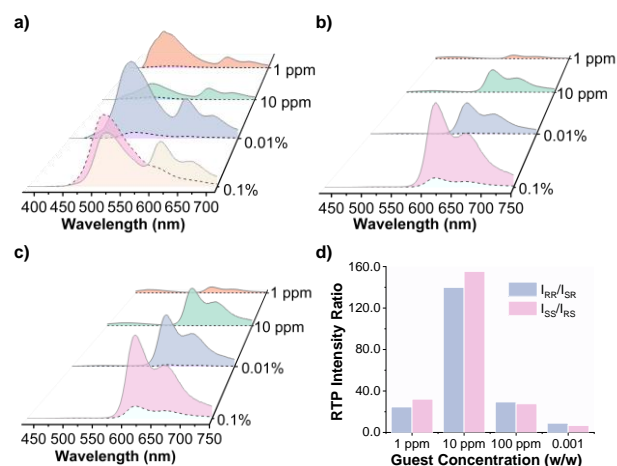


Figure 2. a) Steady-state ($\lambda_{ex} = 365$ nm) and b) delayed emission (DE, $\Delta t = 0.1$ ms, $\lambda_{ex} = 424$ nm) spectra of **R-4FMNNI** (solid border) and **S-4FMNNI** (dash border) guests (w/w = 1 ppm-0.1%) in the **R-4FBrBI** solid chiral selector medium in air at 298 K ($\lambda_{ex} = 365$ nm). c) Delayed emission (DE, $\Delta t = 0.1$ ms) spectra of **R-4FMNNI** (dash border) and **S-4FMNNI** (solid border) guests (w/w = 1 ppm-0.1%) in **S-4FBrBI** solid in air at 298 K ($\lambda_{ex} = 424$ nm). d) The e_{RTP} value (intensity of DE emission at 620 nm) vs. concentration of guest dopants (w/w = 1 ppm-0.1%).

To test the chiral differentiation potential of the system, by using **S-4FMNNI**-doped **R-4FBrBI** (w/w 0.01%) as an example, the RTP spectroscopic changes with **R-4FMNNI** at varying enantiomeric composition were recorded, where S+0%R, S+1%R, S+5%R and S+10%R represent that the ee values, $([S]-[R])/([S]+[R])$, of the partially racemic guest analyte **4FMNNI** compounds are 100%, 98.02%, 90.48% and 81.82%, respectively (Figure 3 and Figure S22). As can be observed, the RTP intensity is enhanced with a higher R-guest proportion. Remarkably, there is a measurable RTP improvement (2-3 \times by tuning the excitation wavelength) between ee values of 100% and 98%, implying the successful distinguishability for an enantiomer (**R-4FMNNI** in this case) lower than 1% from the racemate with the current RTP chiral recognition method. i.e., the method can be used to resolve the enantiomeric composition and an enantiomer impurity with ee > 98%.

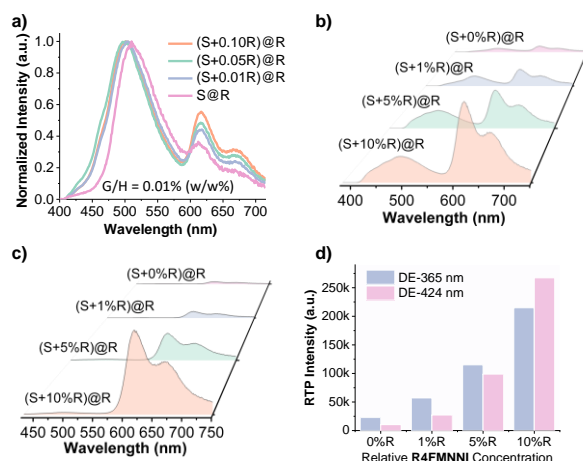


Figure 3. Enantiomer recognition with different ee values: a) Steady-state PL spectra of **R-4FMNNI** dopants (0%-10%) in 0.01% (100 ppm) **S-4FMNNI@R-4FBrBI** solid at air at 298 K ($\lambda_{ex} = 365$ nm). Delayed emission (DE, $\Delta t = 0.1$ ms) spectra of **R-4FMNNI** dopants (0%-10%) in 0.01% **S-4FMNNI@R-4FBrBI** solid at air at 298 K ($\lambda_{ex} = 365$ nm for b) and 424 nm for c)). d) Intensity of DE emission at 618 nm vs. Percentage of **R-4FMNNI** dopants (0%-10%).

Finally, the guest-host RTP chiral recognition method was extended to a different amino compound. Chiral amino alcohols have been extensively used in medicine, racemate resolution and asymmetric synthesis.^[19] Enantioselective recognition of amino alcohols has thus attracted significant research attention in recent years.^[20] Here we show that the same RTP chiral recognition method could be applied to a chiral amino alcohol, using 2-phenylglycinol (Pg) as an example. Following the same protocol, four chiral derivatives (Figure 4a, **R-PgMNNI** and **S-PgMNNI** as guest molecules) and two racemate (Figure S3-4, Figure S50-S67) were synthesized and characterized. When doped at a concentration of 100 ppm, PL spectra (Figure 4b and Figure S25 and S28) reveal that the host-guest system with the same chirality (**R@R** and **S@S**) exhibits more pronounced RTP enhancement over **S@R** or **R@S**, where even the naked eye can readily discriminate the enantioselective luminescence under UV excitation, since **S@R** (or **R@S**) shows cyan emission while the other two are either orange or pink (photos in Figure 4). The DE spectra (Figure 4c) also register an RTP enantioselective enhancement > 10 folds ($I_{RR}/I_{SR} = 11.5$ and $I_{SS}/I_{RS} = 12.7$) with a longer lifetime (Figure 4d, 63.25 ms for **S@S**, 63.36 ms for **R@R**, Table S6). The excitation dependent PL (Figure S23-28) and DE spectra (Figure S29) are analogous to the amino fluorobenzyl compound, suggesting that a similar photophysical process may be involved for the chiral sensing scheme for both amino fluorobenzyl and amino alcohol compounds.

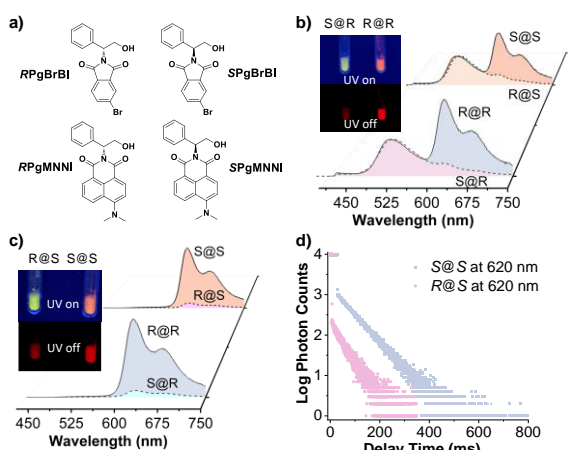


Figure 4. Chiral amino alcohol recognition: a) Molecular structures of chiral amino alcohol derivatives: chemically modified chiral analyte guests (**R-PgMNNI** and **S-PgMNNI**) and chiral selector hosts (**R-PgBrBI** and **S-PgBrBI**) molecules. b) Normalized steady-state PL spectra of two chiral guests (w/w = 100 ppm) in two chiral host solids at 298 K ($\lambda_{\text{ex}} = 380$ nm). Inset: photographs of combinations of two guests in **R-PgBrBI** during and immediately after 365-nm light irradiation. c) Delayed emission (DE, $\Delta t = 0.1$ ms) spectra of two guests (w/w 100 ppm) in two host solids at 298 K ($\lambda_{\text{ex}} = 424$ nm). Inset: photographs of combinations of two guests in **S-PgBrBI** during and immediately after 365-nm light irradiation. d) Time-resolved emission intensity at 620 nm of **R-PgMNNI** and **S-PgMNNI** in the solid-state **R-PgBrBI**.

In summary, we have successfully demonstrated a photoluminescence chiral recognition method by taking advantage of the more sensitive guest-host room-temperature phosphorescence (RTP). We show that by chemically modifying chiral amino compounds into phthalimide selector hosts and naphthalimide analyte guest, an RTP intensity difference of up to 196 folds can be obtained. In combination with fluorescence emission, the dramatic chirality-dependent RTP alters the emission color under UV light, making it easily recognized by the naked eye. To show its application potential, ultratrace analyses were also performed and the method was able to resolve enantiomeric impurity in a partial racemate with an ee value > 98%. Although the method is not yet general, it nevertheless gives one of the best performances in optical chiral recognition so far, and paves way for more generalized, energy-transfer-based guest-host chiral recognition methodologies. The future reports will be focused on detailed mechanistic study for the amplified chirality-dependent RTP, as well as extension to other chemical modification methods for other chiral molecules.

Acknowledgements

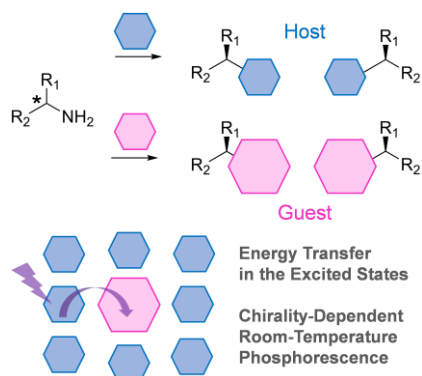
We thank the National Natural Science Foundation (22003063 to B. C. and 21975238 to G. Z.) for financial support. We also thank Prof. Yi Luo for his helpful discussion. CCDC 2150413-2150416 contain the supplementary crystallographic data for this paper.

Keywords: binary doping system • chiral recognition • host and guest • organic chiral solid • room temperature phosphorescence

- [1] a) J. Hu, W. G. Cochrane, A. X. Jones, D. G. Blackmond, B. M. Paegel, *Nat. Chem.* **2021**, *13*, 786-791; b) P. Howlader, E. Zangrando, P. S. Mukherjee, *J. Am. Chem. Soc.* **2020**, *142*, 9070-9078.
- [2] a) Z. Liu, X. Li, H. Masai, X. Huang, S. Tsuda, J. Terao, J. Yang, X. Guo, *Sci. Adv.* **2021**, *7*, eabe4365; b) G. Zhu, O. J. Kingsford, Y. Yi, K.-y. Wong, *J. Electrochem. Soc.* **2019**, *166*, B1226-B1231.
- [3] Z. Du, C. Liu, H. Song, P. Scott, Z. Liu, J. Ren, X. Qu, *Chem* **2020**, *6*, 2060-2072.
- [4] M. E. Matyskiela, S. Couto, X. Zheng, G. Lu, J. Hui, K. Stamp, C. Drew, Y. Ren, M. Wang, A. Carpenter, *Nat. Chem. Biol.* **2018**, *14*, 981-987.
- [5] a) M. Hu, Y.-X. Yuan, W. Wang, D.-M. Li, H.-C. Zhang, B.-X. Wu, M. Liu, Y.-S. Zheng, *Nat. Commun.* **2020**, *11*, 1-10; b) L. Pu, *Acc. Chem. Res.* **2017**, *50*, 1032-1040.
- [6] X. Wu, X. Han, Q. Xu, Y. Liu, C. Yuan, S. Yang, Y. Liu, J. Jiang, Y. Cui, *J. Am. Chem. Soc.* **2019**, *141*, 7081-7089.
- [7] A. Nitti, D. Pasini, *Adv. Mater.* **2020**, *32*, 1908021.
- [8] S. Mishra, A. K. Mondal, E. Z. Smolinsky, R. Naaman, K. Maeda, T. Nishimura, T. Taniguchi, T. Yoshida, K. Takayama, E. Yashima, *Angew. Chem. Int. Ed.* **2020**, *59*, 14671-14676; *Angew. Chem.* **2020**, *132*, 14779-14784.
- [9] G. Qin, Y. Wei, H. Kang, C. Dong, *Anal. Methods* **2012**, *4*, 3928-3931.
- [10] Y. Wei, W.-H. Chan, A. W. Lee, C. W. Huie, *Chem. Commun.* **2004**, 288-289.
- [11] X. Wu, C.-Y. Huang, D.-G. Chen, D. Liu, C. Wu, K.-J. Chou, B. Zhang, Y. Wang, Y. Liu, E. Y. Li, *Nat. Commun.* **2020**, *11*, 1-10.
- [12] X. H. Zhang, Y. Wang, W. J. Jin, *Anal. Chim. Acta.* **2008**, *622*, 157-162.
- [13] a) P. Sutter, S. Wimer, E. Sutter, *Nature* **2019**, *570*, 354-357; b) M. Singh, K. Liu, S. Qu, H. Ma, H. Shi, Z. An, W. Huang, *Adv. Opt. Mater.* **2021**, *9*, 2002197.
- [14] A. S. Carretero, A. S. Castillo, A. F. Gutiérrez, *Crit. Rev. Anal. Chem.* **2005**, *35*, 3-14.
- [15] B. Chen, W. Huang, X. Nie, F. Liao, H. Miao, X. Zhang, G. Zhang, *Angew. Chem. Int. Ed.* **2021**, *60*, 16970-16973; *Angew. Chem.* **2021**, *133*, 17107-17110.
- [16] Y. Lei, W. Dai, J. Guan, S. Guo, F. Ren, Y. Zhou, J. Shi, B. Tong, Z. Cai, J. Zheng, *Angew. Chem. Int. Ed.* **2020**, *59*, 16054-16060; *Angew. Chem.* **2020**, *132*, 16188-16194.
- [17] K. Wen, S. Yu, Z. Huang, L. Chen, M. Xiao, X. Yu, L. Pu, *J. Am. Chem. Soc.* **2015**, *137*, 4517-4524.
- [18] L. Pu, *Angew. Chem. Int. Ed.* **2020**, *59*, 21814-21828; *Angew. Chem.* **2020**, *132*, 21998-22012.
- [19] a) Y.-Y. Zhu, X.-D. Wu, S.-X. Gu, L. Pu, *J. Am. Chem. Soc.* **2018**, *141*, 175-181; b) F. Y. Thanzeel, A. Sripada, C. Wolf, *J. Am. Chem. Soc.* **2019**, *141*, 16382-16387.
- [20] S.-L. Shi, Z. L. Wong, S. L. Buchwald, *Nature* **2016**, *532*, 353-356.

Entry for the Table of Contents

Insert graphic for Table of Contents here.



Guest-host systems exhibit highly enantioselective room-temperature phosphorescence enhancement of up to 196 folds and are applied to chiral recognition for chiral amino compounds with high sensitivity and ultratrace analysis.